European Conference on Computational Fluid Dynamics
ECCOMAS CFD 2006
P. Wesseling, E. Oñate and J. Périaux (Eds)

DEVELOPMENT AND APPLICATION OF GENERALIZED MUSTA SCHEMES

V. A. Titarev[†], E.I. Romenski[*] [1] and E.F. Toro[††]

[†,††] University of Trento, Department of Civil and Environmental Engineering,
Via Mesiano, 77, 38050, Trento, ITALY
e-mails: titarev@mail.ru, toroe@ing.unitn.it
[*] Cranfield University, MK43 0AL, Cranfield, UK
Email: E.Romenskiy@cranfield.ac.uk

Key words: Hyperbolic conservation laws; upwind methods, GFORCE flux, MUSTA fluxes, WENO methods, Euler equations, MHD equations, nonlinear elasticity.

Abstract. *This paper is devoted to the construction of numerical fluxes for hyperbolic systems. We first present a GFORCE numerical flux, which is a weighted average of the Lax-Friedrichs and Lax-Wendroff fluxes. For the linear advection equation with constant coefficient, the new flux reduces identically to that of the Godunov first order upwind method. Then we incorporate GFORCE in the framework of the MUSTA approach,[10,12] resulting in a version that we call GMUSTA. Both the GFORCE and GMUSTA fluxes are extended to multi-dimensional non-linear systems in a straightforward unsplit manner, resulting in linearly stable schemes that have the same stability regions as the straightforward multi-dimensional extension of Godunov's method The schemes of this paper share with the family of centred methods the common properties of being simple and applicable to a large class of hyperbolic systems, but are distinctly more accurate. First-order numerical results are presented for the one-dimensional equations of nonlinear elasticity, magnetohydrodynamics. High-order results are given in the framework of the WENO[8] methods for the two-dimensional Euler equations.*

1 Introduction

Numerical methods for solving non-linear systems of hyperbolic conservation laws via finite volume methods or discontinuous Galerkin finite element methods require, as the building block, a monotone numerical flux. The simplest approach for providing a monotone numerical utilizes a symmetric stencil and does not explicitly make use of wave propagation information, giving rise to centred or symmetric schemes. A more refined approach utilizes wave propagation information through the exact or approximate solution of the Riemann problem, giving rise to Godunov methods. Conventional approximate

[1] On leave from Sobolev Institute of Mathematics, Russian Academy of Sciences, Novosibirsk, Russia

Riemann solvers are usually complex and are not available for many systems of practical interest, such as for models for compressible multi-phase flows. It is thus desirable to construct a numerical flux that emulates the best flux available (upwind) with the simplicity and generality of symmetric schemes.

Here we build upon MUSTA approach,[10,12] which leads to schemes that have the simplicity and generality of symmetric schemes and the accuracy of upwind schemes. First we present a new flux that is an average of symmetric fluxes and which reproduces Godunov's upwind scheme for the model hyperbolic equation. For non-linear systems it is found that this flux gives superior results to those of the whole family of incomplete Riemann solvers that do not explicitly account for linearly degenerate fields. Then we incorporate this flux into the MUSTA multi-staging approach, as predictor and corrector. It is found that the resulting MUSTA schemes reproduce the Godunov upwind scheme for the model hyperbolic equation for any number of stages, including multiple space dimensions. They are linearly stable in two and three space dimensions and the stability region is identical to that of the Godunov upwind method. For non-linear systems the MUSTA scheme with one or two stages gives results that are indistinguishable from those of Riemann solvers, such as the exact Riemann solver or Roe's approximate Riemann solver.

Finally, we assess the schemes on carefully chosen test problems for the multidimensional Euler equations for compressible materials, magneto hydrodynamics and nonlinear elasticity. The results illustrate the accuracy and efficiency of new methods combined with the easy of coding.

2 Numerical fluxes in one spatial dimension

Finite volume and discontinuous Galerkin finite element methods rely on a monotone, first-order intercell numerical flux, the building block of the schemes. Here we are concerned with numerical fluxes in the frame of the finite volume approach. Consider a one-dimensional system of hyperbolic conservation laws

$$\partial_t \mathbf{Q} + \partial_x \mathbf{F}(\mathbf{Q}) = \mathbf{0} \,, \tag{1}$$

where $\mathbf{Q}$ is a vector of m components, the conserved variables, and $\mathbf{F}(\mathbf{Q})$ is the corresponding vector of fluxes. A finite volume method for solving (1) reads as follows:

$$\boldsymbol{U}_i^{n+1} = \boldsymbol{U}_i^n - \frac{\Delta t}{\Delta x}\left(\boldsymbol{F}_{i+1/2} - \boldsymbol{F}_{i-1/2}\right), \tag{2}$$

where $\boldsymbol{U}_i^n$ is an approximation to the cell average and $\boldsymbol{F}_{i+1/2}$ is the numerical flux. The description of the scheme (2) is complete once expressions for the numerical fluxes are provided. Godunov[2] proposed to define the intercell numerical flux $\mathbf{F}_{i+\frac{1}{2}}$ in terms of the

self-similar solution, if available, of the corresponding Riemann problem

$$\begin{aligned} &\partial_t \mathbf{Q} + \partial_x \mathbf{F}(\mathbf{Q}) = \mathbf{0}, \\ &\mathbf{Q}(x,0) = \begin{cases} \mathbf{Q}_i^n = \boldsymbol{U}_L & \text{if} \quad x < 0\,, \\ \mathbf{Q}_{i+1}^n = \boldsymbol{U}_R & \text{if} \quad x > 0\,. \end{cases} \end{aligned} \tag{3}$$

More generally, the numerical flux can be defined as a two-point function of left and right data in the local Riemann problem, namely

$$\boldsymbol{F}_{i+1/2} = \boldsymbol{F}_{i+1/2}(\boldsymbol{U}_L, \boldsymbol{U}_R). \tag{4}$$

In most cases the upwind Godunov-type fluxes cannot be written as an explicit function of $\boldsymbol{U}_L$, $\boldsymbol{U}_R$. Centred fluxes can be written in the form (4), which makes them simple to implement but also rather diffusive as compared to upwind fluxes.

2.1 Centred fluxes

Two classical centred fluxes are the Lax-Friedrichs flux

$$\boldsymbol{F}^{LF}_{i+\frac{1}{2}}(\boldsymbol{U}_L, \boldsymbol{U}_R, \Delta t, \Delta x) = \frac{1}{2}[\boldsymbol{F}(\boldsymbol{U}_L) + \boldsymbol{F}(\boldsymbol{U}_R)] - \frac{1}{2}\frac{\Delta x}{\Delta t}[\boldsymbol{U}_R - \boldsymbol{U}_L] \tag{5}$$

and the two-step Lax-Wendroff flux

$$\boldsymbol{F}^{LW}_{i+\frac{1}{2}}(\boldsymbol{U}_L, \boldsymbol{U}_R, \Delta t, \Delta x) = \boldsymbol{F}(\boldsymbol{U}_{LW})\ , \ \ \boldsymbol{U}_{LW} = \frac{1}{2}[\boldsymbol{U}_L + \boldsymbol{U}_R] - \frac{1}{2}\frac{\Delta t}{\Delta x}[\boldsymbol{F}(\boldsymbol{U}_R) - \boldsymbol{F}(\boldsymbol{U}_L)]\ . \tag{6}$$

Another, more recent, first order centred flux is the FORCE flux[11,13] given by the arithmetic average of the Lax-Friedrichs and Lax-Wendroff fluxes:

$$\boldsymbol{F}^{\text{force}}_{i+\frac{1}{2}}(\boldsymbol{U}_L, \boldsymbol{U}_R, \Delta t, \Delta x) = \frac{1}{2}\boldsymbol{F}^{LW}_{i+\frac{1}{2}}(\boldsymbol{U}_L, \boldsymbol{U}_R, \Delta t, \Delta x) + \frac{1}{2}\boldsymbol{F}^{LF}_{i+\frac{1}{2}}(\boldsymbol{U}_L, \boldsymbol{U}_R, \Delta t, \Delta x). \tag{7}$$

2.2 GFORCE flux

As is well known, centred (or symmetric) fluxes contain no explicit wave propagation information which makes them simple, efficient and applicable to very complex equations, but also quite diffusive and dependent on the Courant number coefficient. In particular, waves associated with linearly degenerate fields, such as contact waves, shear waves and vortices, are poorly resolved.

A simple way of removing the dependence of the truncation error on the reciprocal of the Courant number in the FORCE flux while retaining its simplicity is to use a local time step in (7); this time step is estimated from the data $\boldsymbol{U}_L$, $\boldsymbol{U}_R$.[10] A further improvement, which we call the generalized FORCE (GFORCE) flux, is given by a convex average of (5) and (6), again with the local selection of the time step:

$$\boldsymbol{F}^{GF}_{i+\frac{1}{2}}(\boldsymbol{U}_L, \boldsymbol{U}_R) = \omega \boldsymbol{F}^{LW}_{i+\frac{1}{2}}(\Delta t_g, \Delta x_g) + (1-\omega)\boldsymbol{F}^{LF}_{i+\frac{1}{2}}(\Delta t_g, \Delta x_g), \quad \omega = \frac{1}{1+K_g}. \tag{8}$$

Here $0 < K_g \leq 1$ is a prescribed local Courant number coefficient; usually we take $K_g = 0.9$. The choice $\Omega = 1/2$ gives the modified FORCE flux of.[10] The time step used in the evaluation of the flux is computed from the initial data $\boldsymbol{U}_L$, $\boldsymbol{U}_R$ as

$$\Delta t_g = K_g \Delta x_g / S_{max}. \tag{9}$$

Here S_{max} is the speed of the fastest wave in the local solution. The local cell size Δx_g can be chosen arbitrary due to the self-similar structure of the solution of the conventional Riemann problem. For example, one could take $\Delta x_g \equiv 1$ or $\Delta x_g \equiv \Delta x$. Note, that generally speaking $\Delta t_g \neq \Delta t$.

The GFORCE flux is upwind due to the fact that the nonlinear weight ω in (8) depends on the local wave speed. For the linear advection equation with constant coefficient the proposed flux (8) reproduces the Godunov's upwind flux.

2.3 GMUSTA fluxes

The idea of the multi-stage (MUSTA) Riemann solver[12] is to obtain an upwind numerical flux by evolving in time the initial data in the local Riemann problem. Below we further improve the generalized version of MUSTA, called GMUSTA, as given in.[10,12] Let us introduce a separate spatial domain and corresponding mesh with $2M$ cells: $-M+1 \leq m \leq M$ and cell size δx. The boundary between cells $m = 0$ and $m = 1$ corresponds to the interface position $x = 0$ in (3). Transmissive boundary conditions are applied at numerical boundaries $x_{\pm M+1/2}$ on the grounds that the Riemann - like data extends to $\pm\infty$. We now want to solve this Riemann problem numerically on a given separate mesh and construct a sequence of *evolved* data states $\boldsymbol{Q}_m^{(l)}$, $0 \leq l \leq k$ in such a way, that the final values $\boldsymbol{Q}_0^{(k)}$, $\boldsymbol{Q}_1^{(k)}$ adjacent to the origin are close to the sought Godunov state. Here k is the total number of stages (time steps) on this separate mesh of the algorithm.

The GMUSTA time marching for $m = -M+1, \ldots M$ is organized by using the first-order scheme with the GFORCE flux (8) on the chosen separate mesh:

$$\boldsymbol{U}_m^{(l+1)} = \boldsymbol{U}_m^{(l)} - \frac{\delta t}{\delta x}\left(\boldsymbol{F}_{m+1/2}^{(l)} - \boldsymbol{F}_{m-1/2}^{(l)}\right), \quad \boldsymbol{F}_{m+1/2}^{(l)} = \boldsymbol{F}^{GF}(\boldsymbol{U}_m^{(l)}, \boldsymbol{U}_{m+1}^{(l)}). \tag{10}$$

The time marching procedure is stopped when the required number of stages k is reached. At the final stage we have a pair of values adjacent to the interface position. For the construction of Godunov-type advection schemes one needs a numerical flux at the origin, which for the outlined procedure is given by

$$\boldsymbol{F}_{i+1/2}^{GM} = \boldsymbol{F}_{1/2}^{(k)} = \boldsymbol{F}^{GF}(\boldsymbol{U}_0^{(k)}, \boldsymbol{U}_1^{(k)}). \tag{11}$$

The cell size δx can be chosen arbitrarily due to the self-similar structure of the solution of the conventional Riemann problem. Normally we take $\delta x \equiv 1$. The Courant number coefficient K_{musta} is prescribed by the user; we typically take $K_{musta} = 9/10$. The time step δt is computed from the data $\boldsymbol{U}_m^{(l)}$ according to the conventional formula

$$\delta t = K_{musta} \delta x / S_{max}.$$

with the only difference that S_{max} is computed from all cells in the GMUSTA mesh.

3 First-order one-dimensional examples

In this section we present numerical results of first-order GMUSTA schemes as applied to two hyperbolic systems: MHD and nonlinear elqsticity. As test problems we solve Riemann problems with piece-wise constant initial data:

$$\frac{\partial \boldsymbol{U}}{\partial t} + \frac{\partial \boldsymbol{F}(\boldsymbol{U})}{\partial x} = 0, \quad \boldsymbol{W}(x,0) = \begin{cases} \boldsymbol{W}_L, & x < x_0 \ , \\ \boldsymbol{W}_R, & x > x_0 \ , \end{cases} \tag{12}$$

where x_0 is the position of the discontinuity in initial data. Note that we specify initial data in terms of primitive variables rather than conservative ones to make the presentation more convenient. Transmissive boundary conditions are applied at the boundaries of the domain.

In all calculations we denote the GMUSTA Riemann solvers with k stages as GMUSTA-k.

3.1 Nonlinear elasticity

Three-dimensional processes of elastic media deformation in the Cartesian coordinate system x_i can be described by the complete set of parameters of state such as the velocity vector $\boldsymbol{u} = \{u_i\}$, Eulerian deformation gradient $C = \{c_{ij}\}$, which we also call the Eulerian distortion tensor, and specific entropy S. Other variables, such as material density ρ, the stress tensor σ_{ik} and the specific internal energy e can be represented as functions of the above parameters.

We formulate the governing equations as a first-order hyperbolic system in conservative form using the Eulerian deformation gradient as the parameter of state. This formulation is a straightforward consequence of the thermodynamically compatible system theory developed in.[3,4] Assume that deformation of a medium is uniform along the $x_1 \equiv x$ axis and only one tangential component of the velocity vector is nonzero. In this case the complete set of parameters of state of a medium consists of normal $u = u_1$ and tangential $v = u_2$ components of the velocity vector; $c_{11}, c_{12}, c_{21}, c_{22}$ components of the distortion tensor and entropy S. We adopt the following form of the augmented one-dimensional system:

$$\begin{aligned} \boldsymbol{U} &= (\rho, \ \rho u, \ \rho v, \ \rho c_{12}, \ \rho c_{21}, \ \rho c_{22}, \ \rho(e + u^2/2 + v^2/2))^T \, , \\ \boldsymbol{F}(\boldsymbol{U}) &= (\rho u, \ \rho u^2 - \sigma_{11}, \ \rho uv - \sigma_{21}, \ 0, \ \rho(c_{21}u - c_{11}v)^T, \\ &\qquad \rho(c_{22}u - c_{12}v), \ \rho u(e + (u^2+v^2)/2) - u\sigma_{11} - v\sigma_{21})^T. \end{aligned} \tag{13}$$

The closure relation for the system is the equation of state that defines the specific internal energy e as function of distortion tensor and entropy: $e = e(c_{ij}, S)$. Then density

ρ, strain tensor g_{ij}, stress tensor σ_{ik} and temperature T are given by

$$\rho = \rho_0 / \det C, \quad G = (g_{ij}) = C^{-1*} C^{-1}, \quad \sigma_{ik} = \rho c_{ij} \frac{\partial e}{\partial c_{kj}} = -2\rho g_{ij} \frac{\partial e}{\partial g_{jk}}, \quad T = \frac{\partial e}{\partial S}.$$

Here ρ_0 is a constant mass density in the reference unstressed state.

For an isotropic medium the equation of state must be a function of three independent invariants I_1, I_2, I_3 of strain tensor which can be chosen in different ways. We shall use

$$I_1 = \mathrm{tr} G = g_{11} + g_{22} + g_{33}, \qquad I_3 = \det G = \left(\rho/\rho_0\right)^2,$$

$$I_2 = (g_{11} g_{22} - g_{12} g_{21}) + (g_{22} g_{33} - g_{23} g_{32}) + (g_{33} g_{11} - g_{31} g_{13}).$$

Note that for the two-dimensional case we have to set $g_{33} \equiv 1$. The equation of state used in the present paper is given as the sum of three terms of which two correspond to the hydrodynamic part of the internal energy and one corresponds to the shear deformation:[7]

$$e = \frac{K_0}{2\alpha^2}(I_3^{\alpha/2} - 1)^2 + c_V T_0 I_3^{\gamma/2}(e^{S/c_V} - 1) + \frac{B_0}{2} I_3^{\beta/2}(I_1^2/3 - I_2). \tag{14}$$

Here K_0 and B_0 are bulk and shear modulus, c_V is heat capacity at constant volume, α, β, γ are constants characterizing nonlinear dependence of sound speeds and temperature on the mass density. As the material for test computations we take copper with the following constants in the equation of state:

$$\rho_0 = 8.9\ g/cm^3,\ K_0 = c_0^2 - \frac{4}{3} b_0^2,\ B_0 = b_0^2,\ c_0 = 0.46\ cm/ms,\ b_0 = 0.21\ cm/ms,$$

$$T_0 = 300\ K,\ c_v = 0.4 \cdot 10^{-4}\ \frac{g}{ms\ K},\ \alpha = 1.0,\ \beta = 3.0,\ \gamma = 2.0.$$

Nonzero components of the strain tensor g_{ij} are

$$g_{11} = f_{11}^2 + f_{21}^2, \quad g_{12} = g_{21} = f_{11} f_{12} + f_{21} f_{22}, \quad g_{22} = f_{12}^2 + f_{22}^2,$$

where the entries f_{ij} of the C^{-1} matrix are given by

$$(f_{11},\ f_{12},\ f_{21},\ f_{22}) = (c_{22}, -c_{12},\ -c_{21}, c_{11})/\mathrm{det} C, \quad \mathrm{det} C = c_{11} c_{22} - c_{12} c_{21}.$$

The mass density can be represented as a function of either c_{ij} or g_{ij}:

$$\rho = \rho_0 / \mathrm{det} C = \rho_0 \sqrt{g_{11} g_{22} - g_{12} g_{21}}.$$

The components of the stress tensor are given by:

$$\begin{aligned}
\sigma_{11} &= -2\rho g_{11} \frac{\partial E}{\partial g_{11}} - 2\rho g_{12} \frac{\partial E}{\partial g_{21}}, \\
\sigma_{12} = \sigma_{21} &= -2\rho g_{11} \frac{\partial E}{\partial g_{12}} - 2\rho g_{12} \frac{\partial E}{\partial g_{22}}, \\
\sigma_{22} &= -2\rho g_{21} \frac{\partial E}{\partial g_{12}} - 2\rho g_{22} \frac{\partial E}{\partial g_{22}}.
\end{aligned}$$

Finally, the system should satisfy the compatibility conditions which in the one-dimensional case read as follows:

$$\rho c_{11} = \text{const}, \quad \rho c_{12} = \text{const}. \tag{15}$$

3.2 Stationary contact discontinuity

We solve the Riemann problem with initial data corresponding to a stationary contact discontinuity defined in a computational domain $[0:1]$:

$$\begin{aligned} \boldsymbol{W}_L &= (0, 0, 1.156276139, 0.034688284, 0.093190648, 1.002195719, 0.001), \\ \boldsymbol{W}_R &= (0, 0, 1, 0.03, 0.02, 1, 0), \end{aligned} \tag{16}$$

and $x_0 = 0.5$. The exact solution is given by $\boldsymbol{W}(x,t) \equiv \boldsymbol{W}(x,0)$. We run the schemes up to the output time $t = 1$ on a mesh of 100 cells using a CFL coefficient $CFL = 0.9$. This corresponds to approximately 530 time steps.

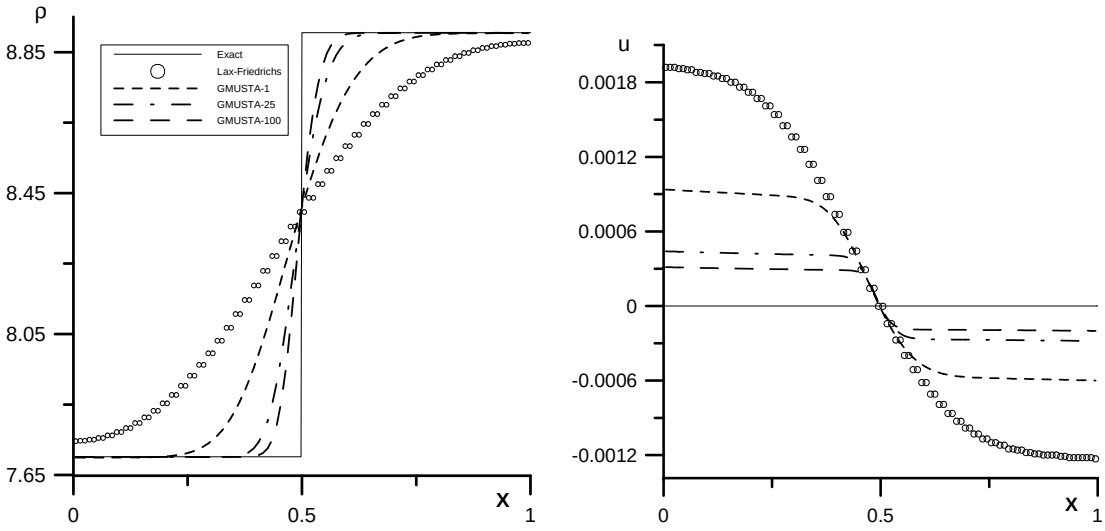

Figure 1: Stationary contact discontinuity. First-order scheme with the GMUSTA flux and different number of stages. The solid line represents the exact solution.

Fig. 1 shows computed results for schemes with Lax-Friedrichs flux as well GMUSTA flux with different number of stages. Symbols correspond to numerical solution of the method under discussion whereas the solid line corresponds to the exact solution. We see that the Lax-Friedrichs scheme is exceedingly diffusive, with a typical 'pairing' of cells. In particular, the computed normal velocity is not zero in the whole computational domain. Additionally, the computed normal stress σ_{11}, not shown in the figures, deviates from its exact value by about 5–10%. The GMUSTA is a significantly more accurate scheme. When the number of stages increases the GMUSTA results seem to approach slowly a limiting profile, which is however different from the exact one.

3.3 Three-wave shock-tube problem

The initial data satisfying the compatibility conditions (15) is given by

$$\boldsymbol{W}_L = (0, 0, 0.95, 0, 0, 1, 0.001), \quad \boldsymbol{W}_R = (0, 0, 1, 0, 0, 1, 0), \tag{17}$$

and $x_0 = 0.5$. The structure of the solution consists of (from left to right) a left travelling rarefaction wave, a right-travelling contact discontinuity with velocity and a right-travelling shock wave.

We run the schemes up to the output time $t = 0.06$ on a mesh of 100 cells and a CFL coefficient $CFL = 0.9$. Fig. 2 contains the results of all fluxes. Again symbols correspond to numerical solution of the method under discussion whereas the solid line corresponds to the exact solution. Overall, the least accurate is the scheme, which produces very smeared profiles of all quantities with very typical 'pairing' of cells. GFORCE and GMUSTA-1 fluxes are visibly more accurate for all waves. We note that these two fluxes are of virtually identical accuracy at the shock front and across the smooth rarefaction wave but differ for the contact discontinuity, for which GMUSTA-1 is more accurate.

4 Ideal Magnetohydrodynamics

We solve the one-dimensional MHD equations

$$\left.\begin{gathered} \partial_t \mathbf{Q} + \partial_x \mathbf{F}(\mathbf{Q}) = \mathbf{0}\,, \\ \mathbf{Q} = \begin{bmatrix} \rho \\ \rho u \\ \rho v \\ \rho w \\ E \\ B_y \\ B_z \end{bmatrix}, \quad \mathbf{F} = \begin{bmatrix} \rho u \\ \rho u^2 + p_T - B_x^2 \\ \rho uv - B_x B_y \\ \rho uw - B_x B_z \\ (E + p_T)u - B_x(uB_x + vB_y + wB_z) \\ B_y u - B_x v \\ B_z u - B_x w \end{bmatrix}, \end{gathered}\right\} \tag{18}$$

where $\mathbf{B} = (B_x, B_y, B_z)$ is the magnetic field,

$$p_T = p + \frac{1}{2}\mathbf{B}^2\,, \quad E = \frac{p}{(\gamma - 1)} + \frac{1}{2}\rho(u^2 + v^2 + w^2) + \frac{1}{2}\mathbf{B}^2\,, \tag{19}$$

p is the gasdynamical pressure, ρ is density, E is total energy and u, v, w are velocity components.

We solve the Riemann problem for (18) with the parameters corresponding to the first test problem of Brio and Wu.[1] The computational domain is the interval $[-0.5 : 0.5]$, the ratio of specific heats is set to $\gamma = 2$. The initial conditions are as follows:

$$B_x = 0.75, \quad u = v = w = 0, \quad (\rho, p, B_y, B_z) = \begin{cases} (1.0, 1.0, +1.0, 0.0) & x < 0\,, \\ (0.125, 0.1, -1.0, 0.0) & x > 0\,. \end{cases} \tag{20}$$

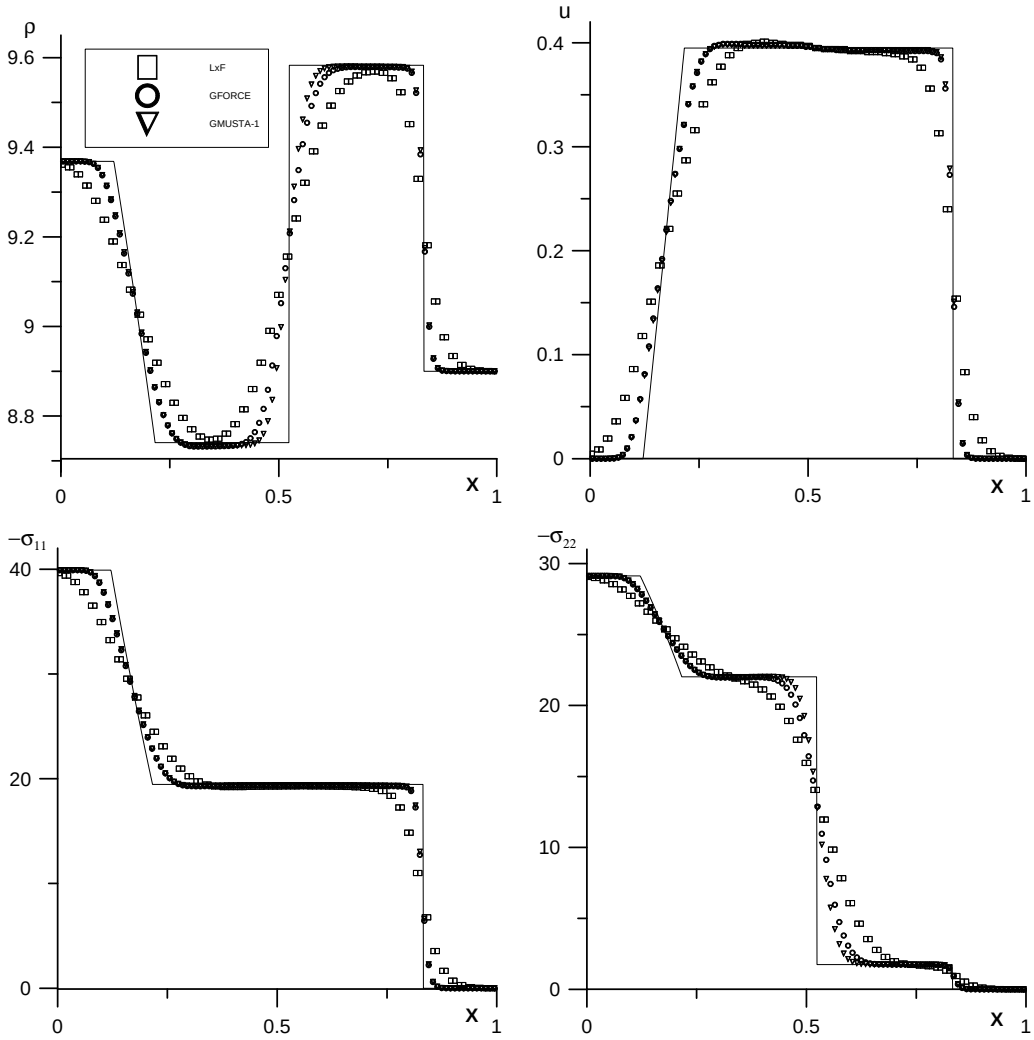

Figure 2: Three-wave shock-tube problem. First-order scheme with the Lax-Friedrichs, GFORCE and GMUSTA-1 fluxes.

We obtain a reference solution of (18) with the initial data (20) by applying the GMUSTA scheme on the very fine mesh of 10000 cells. Comparing this reference solution with those reported in the current literature,[1,5,6] we observe that a structure of the solution accepted as correct is obtained.

Figs. 3-4 show computed results using the schemes presented in this paper using a mesh of 400 cells and a CFL coefficient $CFL = 0.9$. The GFORCE results are shown by the dashed line, the GMUSTA-1 results are shown by symbols and the reference solution is shown by the full line. We consider both numerical schemes to give satisfactory results, all main features of the solution are captured. As expected, the GMUSTA-1 results are more accurate than the GFORCE results, particularly for the contact wave.

For comparison with other simple methods, we have also computed the solution using

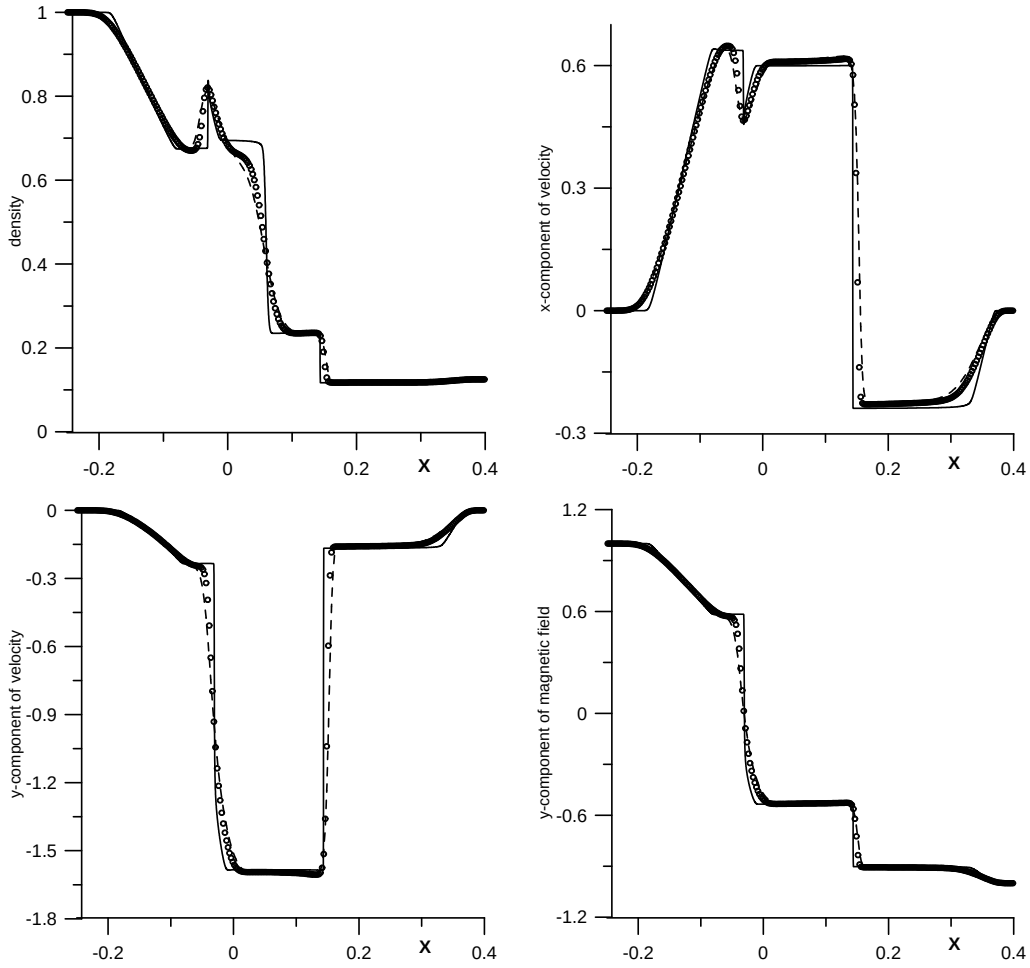

Figure 3: **Brio and Wu MHD Test Problem.** GFORCE (dashed line) and GMUSTA-1 (symbols) results with CFL=0.9 and 400 cells. Reference solution shown by full line.

the Lax-Friedrichs scheme and the FORCE scheme, which is algebraically equivalent to the two-step staggered grid Lax-Friedrichs method. The results for CFL=0.9 omitted here show that the schemes of this paper are significantly more accurate, for all waves in the solution. Moreover, the observed difference in accuracy increases for small Courant numbers. Fig. 4 shows a comparison of solutions for $CFL = 0.2$ and 400 cells. Large differences are observed. The two centred methods, Lax-Friedrichs and FORCE, are badly affected by small CFL numbers. The significant improvement from Lax-Friedrichs to GFORCE and GMUSTA, specially for small CFL numbers is due to the fact that the local truncation error of our new schemes does not depend on the reciprocal of the time step. As a result, the accuracy of the GFORCE scheme, and thus GMUSTA, does not degrade much for small Courant numbers.

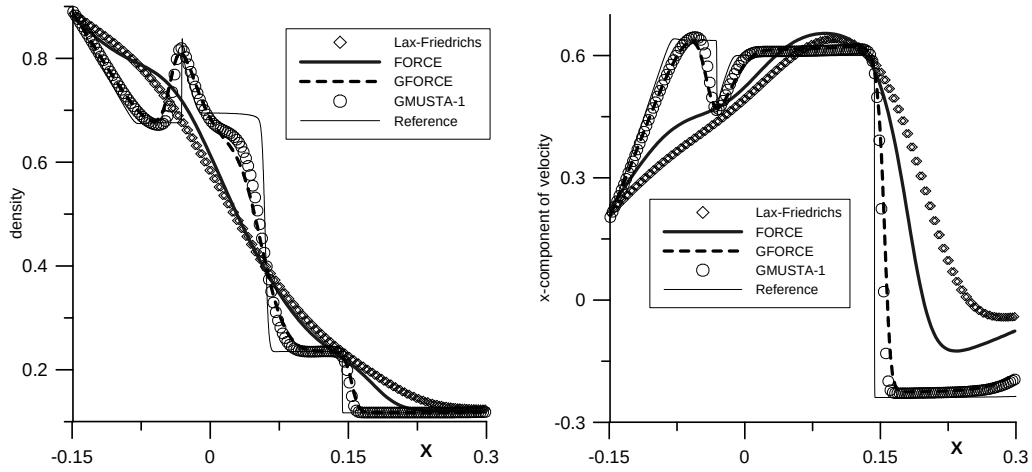

Figure 4: **Brio and Wu MHD Test Problem.** Numerical solutions with CFL=0.2 and 400 cells. Reference solution shown by full line.

4.1 Multiple Space Dimensions and High Order

The numerical fluxes proposed in this paper can be used directly in *unsplit, or simultaneous updating* finite volume schemes as well as in the frame of discontinuous Galerkin approaches to obtain schemes of higher order of accuracy, along with various ways of constructing non-oscillatory versions of the schemes. In their simplest form, the resulting multi-dimensional schemes use the appropriate one-dimensional fluxes in the direction normal to the cell interface at the appropriate integration point. In this framework, any existing finite volume code based on some Riemann solver can be easily modified by replacing the numerical flux by the GMUSTA flux of this paper.

The GMUSTA fluxes can be used to construct schemes of very high order of accuracy in space and time. Here we illustrate this in the frame of WENO schemes with Runge-Kutta time stepping, as applied to the two-dimensional Euler equations for ideal gases. We use GMUSTA as the building block in the state-of-art weighted essentially non-oscillatory (WENO) schemes. For a detailed description of finite-volume WENO schemes in two space dimensions see[8] and references therein and[9] for the three dimensional extension.

Generally speaking, different two-point numerical flux numerical fluxes can be used as the building block for WENO schemes. For example, Shi and Shu[8] use the Rusanov flux as the building block. In this paper we replace the conventional bulding block by the two-point GMUSTA flux and denote the resulting scheme as the WENO-GMUSTA scheme. We use fifth-order spatial reconstruction and third-order time integrations, see[8,9] for details. We note that in two space dimensions the variant of the WENO scheme from[9] is different from that of[8] in that it uses a two-point Gaussian quadrature instead of a three point quadrature.

As an example, we consider the double Mach reflection[14] for the two-dimensional com-

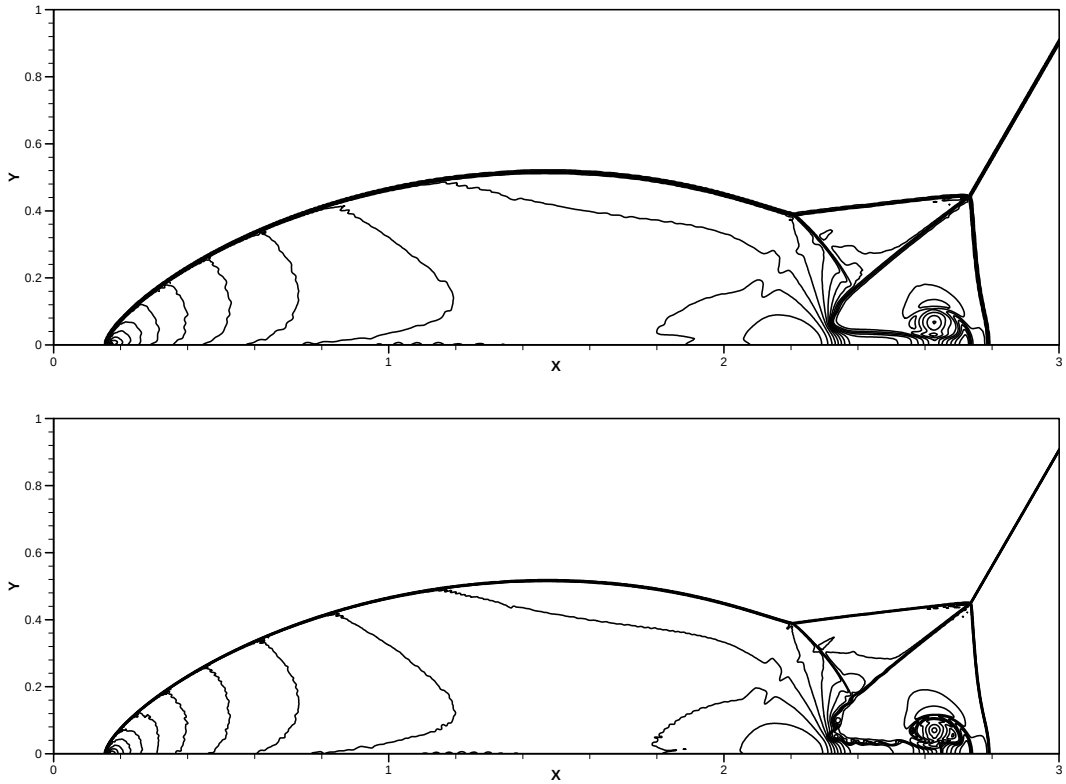

Figure 5: **Double Mach Reflection Test Problem.** Results from the WENO-GMUSTA-1 scheme. Meshes of 960×240 (top) and 1920×480 (bottom) cells are used. A number of 30 contour lines from 2 to 22 are displayed.

pressible Euler equations for an ideal gas:

$$\partial_t \mathbf{Q} + \partial_x \mathbf{F}(\mathbf{Q}) + \partial_y \mathbf{G}(\mathbf{Q}) = \mathbf{0} \tag{21}$$

where the vector of conserved variables $\mathbf{Q}$ and fluxes $\mathbf{F}$, $\mathbf{G}$ are given by

$$\mathbf{Q} = \begin{pmatrix} \rho \\ \rho u \\ \rho v \\ E \end{pmatrix}, \quad \mathbf{F} = \mathbf{Q}u + \begin{pmatrix} 0 \\ p \\ 0 \\ pu \end{pmatrix}, \quad \mathbf{G} = \mathbf{Q}v + \begin{pmatrix} 0 \\ 0 \\ p \\ pv \end{pmatrix} \tag{22}$$

$$p = (\gamma - 1)(E - \frac{1}{2}\rho(u^2 + v^2))$$

and $\mathbf{S} = \mathbf{0}$. Here ρ, u, v, p and E are density, components of velocity in the x and y coordinate directions, pressure and total energy, respectively; γ is the ratio of specific heats. We use $\gamma = 1.4$ throughout. The formulation of the Mach reflection problem, computational setup and detailed discussion of the flow physics can be found in.[14] Fig. 5 shows numerical results from the WENO scheme with the GMUSTA-1 flux of this paper

on two meshes: 960×240 and 1920×480 cells. We observe that the scheme produces the flow pattern generally accepted in the present literature [8,14] as correct, on all meshes. At a given output time a complicated flow pattern contains two Mach shocks, two slip surfaces and a jet. All discontinuities are well resolved by the scheme and correctly positioned.

5 Conclusion

We have first presented a new upwind numerical flux, called GFORCE, that is a generalization of the FORCE symmetric flux. Then we have incorporated this flux into the MUSTA framework. Unlike conventional upwind methods using Riemann solvers, our schemes are applicable to general systems of hyperbolic conservation laws. For a given vector of conserved variables, a corresponding flux vector and appropriate closure relations, the proposed MUSTA numerical flux is most easily computed. For multi-dimensional problems the unsplit versions of the schemes are linearly stable, unlike those of well-known symmetric fluxes such as Lax-Friedrichs and FORCE.

The performance of the new schemes has been demonstrated via the MHD and Euler equation as well as nonlinear elasticity equations. The results demonstrate that our schemes are clearly superior to conventional centred methods.

Acknowledgements. The first author also acknowledges the financial support provided by the PRIN programme (2004-2006) of Italian Ministry of Education and Research (MIUR). The second author acknowledges MIUR for the partial financial support provided during his stay as a visiting professor at the Department of Civil and Environmental Engineering, University of Trento. The third author acknowledges the support of an EPSRC grant, as senior visiting fellow (Grant GR N09276) at the Isaac Newton Institute for Mathematical Sciences, University of Cambridge, UK, 2003.

REFERENCES

[1] M. Brio and C.C. Wu. An upwind differencing scheme for the equations of ideal magnetohydrodynamic equaitons. *J. Comput. Phys.*, 75, 1988.

[2] S.K. Godunov. A finite difference method for the computation of discontinuous solutions of the equations of fluid dynamics. *Mat. Sbornik*, 47:357–393, 1959.

[3] S.K. Godunov and E.I. Romenski. Thermodynamics, conservation laws, and symmetric forms of differential equations in mechanics of continuous media. In *Computational Fluid Dynamics Review 95*, pages 19–31. John Wiley, NY, 1995.

[4] S.K. Godunov and E.I. Romenski. *Elements of Continuum Mechanics and Conservation Laws.* Kluwer Academic/ Plenum Publishers, 2003.

[5] G.-S. Jiang and C.C. Wu. A high order WENO finite-difference scheme for the equations of the ideal magnetohydrodynamics. *J. Comput. Phys.*, 150:561–594, 1999.

[6] A.G. Kulikovskii, N. V. Pogorelov, and A. Yu. Semenov. *Mathematical Aspects of Numerical Solution of Hyperbolic Systems*. Chapman and Hall, 2002. Monographs and Surveys in Pure and Applied Mathematics, Vol. 118.

[7] E. Romenski. Numerical method for 2d equations of nonlinear elasto-plastic Maxwell media. In *Proc. Inst. Math. Akad. Nauk USSR, Sib. Otd.*, volume 18, pages 83–100, 1990. in Russian.

[8] J. Shi, C. Hu, and C.-W. Shu. A technique for treating negative weights in WENO schemes. *J. Comput. Phys.*, 175:108–127, 2002.

[9] V.A. Titarev and E.F. Toro. Finite-volume WENO schemes for three-dimensional conservation laws. *J. Comput. Phys.*, 201(1):238–260, 2004.

[10] V.A. Titarev and E.F. Toro. Musta schemes for multi-dimensional hyperbolic systems: analysis and improvements. *International Journal for Numerical Methods in Fluids*, 49(2):117–147, 2005.

[11] E.F. Toro. On Glimm-related schemes for conservation laws. *Technical Report MMU-9602, Department of Mathematics and Physics, Manchester Metropolitan University, UK.*, 1996.

[12] E.F. Toro. Multi-stage predictor-corrector fluxes for hyperbolic equations. *Preprint NI03037-NPA. Isaac Newton Institute for Mathematical Sciences, University of Cambridge, UK*, 2003.

[13] E.F. Toro and S.J. Billett. Centred TVD schemes for hyperbolic conservation laws. *IMA J. Numerical Analysis*, 20(1):47–79, 2000.

[14] P. Woodward and P. Colella. The numerical simulation of two-dimensional fluid flow with strong shocks. *J. Comput. Phys.*, 54:115–173, 1984.